

## **Phase-Shift-Controlled Active Boost Rectifier with Soft Switching**

**Morthala Suresh Reddy**

**M.Tech,**

**Anurag Engineering College.**

**V.Achireddy**

**M.Tech,**

**Anurag Engineering College.**

### **ABSTRACT:**

High productivity and high power thickness can be achieved with a dc–dc transformer by working all the switches at a settled half obligation cycle. Be that as it may, the yield voltage of the dc–dc transformer can't be directed. Novel rectifiers named dynamic help rectifiers (ABRs) are proposed in this paper. Essentially, an ABR is made out of a conventional diode rectifier and a bidirectional switch. By receiving stage shift control between the essential and optional side switches, the yield voltage direction can be accomplished while acquainting the ABR with a dc–dc transformer. Subsequently, a group of novel delicate exchanging dc–dc converters is gathered. At the point when the proposed converter works in the delicate exchanging ceaseless conduction mode, zero-voltage-exchanging (ZVS) execution for all the essential and optional side switches is accomplished.

At the point when the converter works in the dis-consistent conduction mode, zero current exchanging (ZCS) for the essential side switches and ZVS for the optional side switches are accomplished. Besides, the diode reverse-recuperation issue is lightened by utilizing the ABR and stage shift control plan. For instance, the full-connect converter with voltage doubler ABR is broke down to confirm the proposed ABR idea and converters. The operation standards, voltage change proportion, and yield attributes are examined inside and out. At last, test results are given to confirm the possibility and viability.

### **Index Terms:**

Active boost rectifier (ABR), DC–DC converter, full-bridge converter (FBC), soft switching, voltage doubler (VD).

### **I. INTRODUCTION:**

With fast advancements of renewable vitality, shrewd network, and electric vehicles, segregated dc–dc converters have been generally utilized as a part of various applications to meet the prerequisites of galvanic confinement and/or voltage transformation proportion [1], [2]. For further enhancements on execution of proficiency, thickness, and electromagnetic clamor, some delicate exchanging dc–dc converters have been proposed for different applications to defeat the impediments in hard-exchanging dc–dc converters [3]–[25]. Among them, the stage move full-connect converter (FBC) is more alluring on the grounds that it can accomplish zero voltage exchanging (ZVS) for all the dynamic switches by embracing stage shift regulation. Notwithstanding, as of recently, despite everything it experiences high voltage ringing and turn around recuperation on the optional side rectifier diodes, constrained ZVS range, circling current-related force misfortune, and obligation cycle misfortune.

The converse recuperation issue of the rectifier diodes turns out to be considerably more genuine in high-yield voltage and high-control applications. Various enhancements have been proposed to tackle these issues. For the most part, some extra segments are acquainted with sup-press the circling streams and mitigate the converse recuperation issue. Case in point, a helper inductor, a transformer, or a winding is acquainted with reuse the vitality in [6]–[15]. In [15], two dynamic changes are acquainted with the auxiliary side rectifier to tackle the opposite recuperation issue, yet the punishment is an extra conduction misfortune. As of late, the double dynamic scaffold topology draws in awesome interest since it can understand ZVS for all the force switches [16]–[19].

In any case, the restricted ZVS extent and high circling streams at light load make this converter unsatisfactory for wide voltage/load range applications. Another attractive answer for the separated dc–dc power change is the LLC full converter [20]–[22]. By outlining and selecting a proper operation district, delicate exchanging of all the dynamic switches and rectifier diodes over a wide load extent can be accomplished with the LLC thunderous converter. Notwithstanding, recurrence balance makes the exact demonstrating of the LLC converter hard to accomplish, furthermore confounds the configuration of attractive components [21]. Additionally, the full tank in the LLC converter ought to be outlined painstakingly also to accomplish high effectiveness, which remains a test for this sort of converter [22].

Then again, the obligation cycle of a dc–dc transformer, which is an open-circle controlled secluded dc–dc converter, is altered at half. Therefore, delicate exchanging of all the force switches can be constantly accomplished by using the spillage or polarizing inductance [23]. Consequently, high productivity and high power lair sity can be effectively accomplished. In any case, the yield voltage/force of a dc–dc transformer can't be managed. In the event that the yield voltage of a dc–dc transformer can be managed, high proficiency might be effortlessly accomplished. To accomplish the objective specified already, this paper proposes the dynamic support rectifier (ABR) idea. The ABR circuit is acquainted with the dc–dc transformer topology to actualize yield voltage/power direction. Accordingly, a group of wide-range delicate exchanging detached dc–dc converters is gathered.

The significant preferred standpoint of the proposed converters is that the ZVS for all the dynamic switches can be accomplished in a wide load range. Above all, these converters can take out the opposite recuperation issue of rectifier diodes, which is extremely basic for high-productivity applications. This paper is composed as takes after.

In Section II, the fundamental thoughts to determine delicate exchanging dc–dc converters in light of the ABR idea are proposed with a group of novel converters given. For instance, a novel FBC with voltage-doubler (VD) ABR is investigated in subtle element to confirm the proposed topology in Section III. Test results are displayed in Section IV. At long last, Section V finishes up this paper.

**II. PROPOSED DC–DC CONVERTERS BASED ON THE ABR**

**A. Concept of an ABR**

For instance, a FBC with a VD rectifier appeared in Fig. 1 is utilized to depict the idea of an ABR. When this converter works as a dc transformer, the obligation cycles of all the switches are altered at 0.5. The voltage-source full-connect inverter, which is made out of a dc info voltage source  $U_{in}$  and four switches  $S_1 - S_4$ , creates an air conditioner square-wave voltage  $u_p$ , applying to the essential twisting of the transformer. Hence, the converter appeared in Fig. 1 can be spoken to by the one appeared in Fig. 2(a). For straightforwardness, considering a perfect transformer  $T$  with turns a proportion of 1, this circuit can be further rearranged to an uncontrolled rectifier, as appeared in Fig. 2(b). Clearly the yield voltage can't be directed if the obligation cycles of all the switches are settled at 0.5.

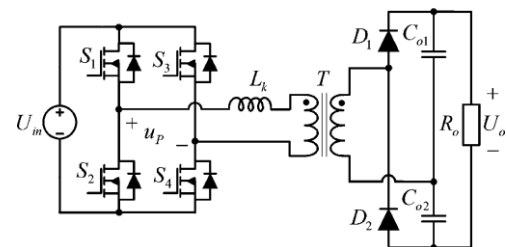


**Fig. 1. Topology of a full-bridge converter with voltage-doubler rectifier.**

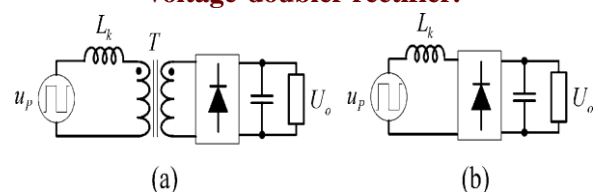


**Fig. 2. Simplified circuits of the full-bridge converter shown in Fig. 1: (a) including the transformer and (b) excluding the transformer.**

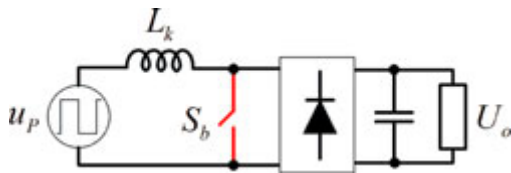


Fig. 3. Principle circuit of the ABR.

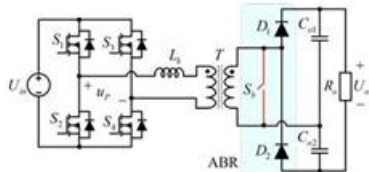


Fig. 4. New full-bridge converter with voltage-doubler ABR.

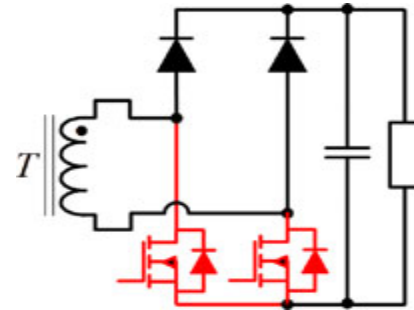


Fig. 8. Simplified full-bridge ABR.

B. To make the yield voltage controllable, a bidirectional switch  $S_b$  can be acquainted with the circuit of Fig. 2(b), then a standard circuit of ABR is determined, as appeared in Fig. 3, where a Boost circuit is worked by the inductor  $L_k$ , switch  $S_b$ , and amending diodes. This circuit is like the ordinary force element rectification support converter [24], [25]. Subsequently, the yield voltage can be controlled by the bidirectional switch  $S_b$ . In this paper, the rectifier made out of the dynamic bidirectional switch  $S_b$  and diodes is named ABR. It is straightforward that the yield voltage of a dc transformer can be controlled by enhancing the uncontrolled diode rectifier to an ABR. For instance, when we apply the ABR to the FBC of Fig. 1, another circuit can be inferred, as appeared in Fig. 4.

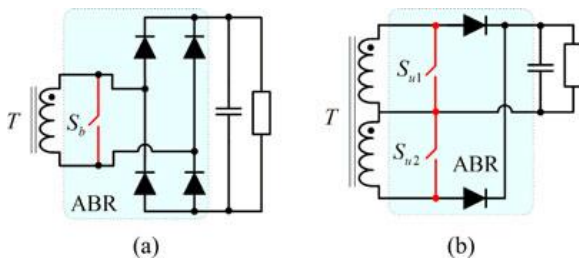


Fig. 5. Topologies of ABR derived from (a) full-bridge and (b) center-tapped diode-rectifiers.

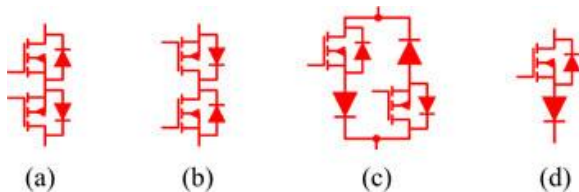


Fig. 6. (a)–(c) Realizations of bidirectional switch and (d) unidirectional switch

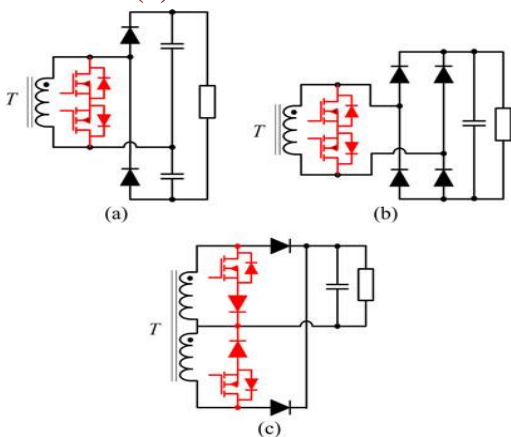


Fig. 7. Derived ABR topologies: (a) voltage-doubler, (b) full-bridge, and (c) center-tapped

### C. Family of DC–DC Converters Based on ABR

#### 1) Circuits of ABR:

In the investigation previously mentioned, an ABR circuit has been inferred in view of a routine VD diode rectifier. This idea can likewise be connected to the routine full-extension and full-wave diode rectifiers, as appeared in Fig. 5. It ought to be noticed that, as appeared in Fig. 5(b), in light of the fact that the transformer has two auxiliary windings, two unidirectional switches  $S_{u1}$  and  $S_{u2}$ , rather than one bidirectional switch, are acquainted with manufacture an ABR. A bidirectional switch can be acknowledged through the mix of MOSFETs and diodes, while a unidirectional switch can be acknowledged however an arrangement association of a MOSFET and a diode.

Some conceivable acknowledge of the bidirectional and unidirectional switches are outlined in Fig. 6. In light of these switches, a group of ABR circuits can be inferred. Some illustration topologies are appeared in Fig. 7. Then again, for the full-connect diode rectifier, a bidirectional switch which is paralleled with the transformer winding can likewise be worked by supplanting the two diodes in the rectifier with two MOSFETs. Accordingly, streamlined full-connect ABR topologies can be determined and appeared in Fig. 8, where the bidirectional switches have been highlighted with red shading. Clearly two diodes can be diminished contrasted with the Fig. 7(b).

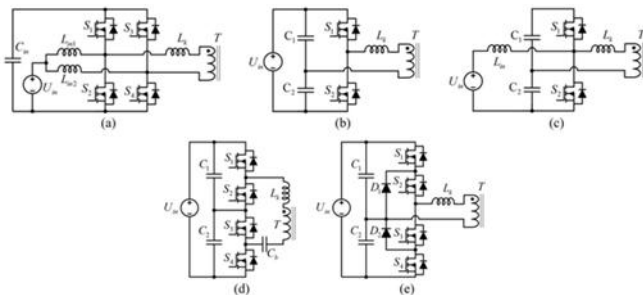


**Fig.9. Topologies of primary side circuits: (a) boost full-bridge, (b) half-bridge, (c) boost half-bridge, (d) and (e) three-level.**

**2).Primary-Side Circuits:**

As showed in Fig. 2, the primary-side circuit ought to have the capacity to create an air conditioner square-wave voltage. Notwithstanding the voltage-sourced full-connect topology, there are numerous different determinations for the essential side circuit. A portion of the topologies, including the support full-connect, halfbridge, help half-extension, and three-level topology, have been appeared in Fig. 9.

**3) New DC-DC Converter Family:**

A group of new dcdconverter topologies can be determined by joining the ABR circuits appeared in Figs. 7 and 8 and the essential side circuits appeared in Fig. 9. A portion of the cases are appeared in Fig. 10. It is found that the working standards and execution of the topology appeared in Fig. 10(d) have been investigated in [26] and [27], which can confirm the achievability and preferences of this topology, and

demonstrate the adequacy of the ABR idea proposed in this paper. It ought to be noticed that, albeit a few circuits have been proposed and dissected, the topological strategy of this topology family has never been brought up methodically, which is the principle commitment of this paper.

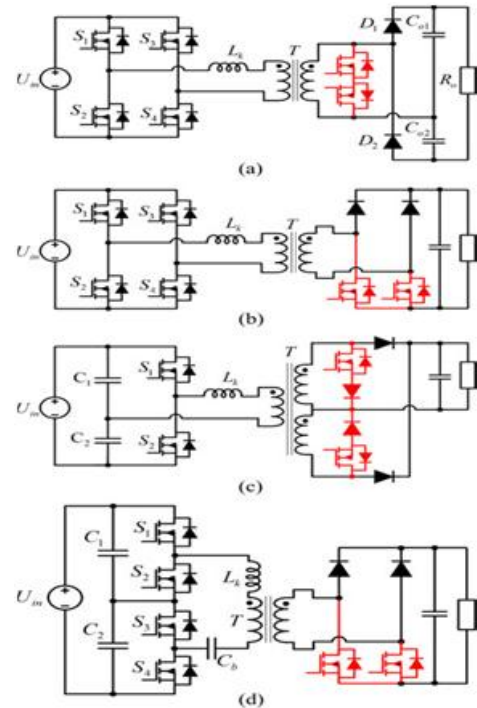


**Fig. 10. New DC-DC converter topologies based on the ABRs.**

**III. ANALYSIS ON THE FBC WITH VOLTAGE-DOUBLER ABR**

One of the proposed topology, the FBC with VD ABR, is taken for instance to be broke down in this area to confirm the achievability of the proposed topologies.

**A. Operational Principle:**

The FBC-VD-ABR is redrawn in Fig. 11, where all the switches on the essential and auxiliary sides have a steady obligation cycle of 0.5. S1 and S4 are constantly turned ON/OFF at the same time, and the same with S2 and S3. A stage shift edge between the essential and auxiliary side dynamic changes is utilized to manage the yield force and voltage. Lf remains for the aggregate of the transformer spillage inductance and outer inductor.

The yield arrangement capacitors  $C_{o1}$  and  $C_{o2}$  have the same capacitance and are sufficiently substantial to clasp the voltage hassles of the auxiliary side changes and diodes to half of the yield voltage.  $u_{D S1}$ ,  $u_{D S4}$ , and  $u_{D S6}$  are the channel to source voltages of  $S_1$ ,  $S_4$ , and  $S_6$ , separately.  $u_P$  and  $u_S$  are the voltages on the essential side and optional side of the transformer. Also,  $i_L$  is the essential current coursing through the transformer with the positive heading appeared in Fig. 11. A legitimate dead time is vital for the essential side changes to accomplish ZVS and maintain a strategic distance from shot-through of the exchanging spans. To rearrange the examination, the parasitic capacitance of MOSFET is overlooked and the transformer is thought to be perfect.

The normalized voltage gain  $G$  is defined as

$$G = \frac{NU_o}{2U_{in}} \quad (1)$$

where  $U_{in}$ ,  $U_o$ , and  $N$  are the input voltage, output voltage, and transformer turns ratio  $n_p / n_s$ , respectively. The phase shift  $\phi$  is defined as the phase difference between  $S_1$  gate signal and  $S_6$  gate signal. Because this phase shift serves the same function as duty cycle in a PWM converter, we define duty cycle  $D$

$$D = \frac{\phi}{\pi} \quad (2)$$

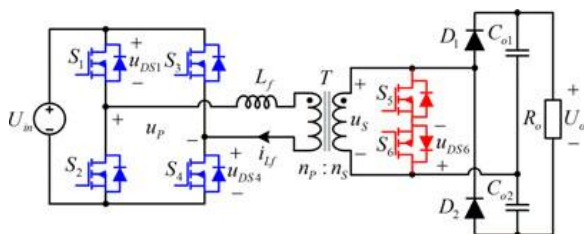


**Fig. 11. Proposed full-bridge converter with voltage-doubler active boost rectifier.**

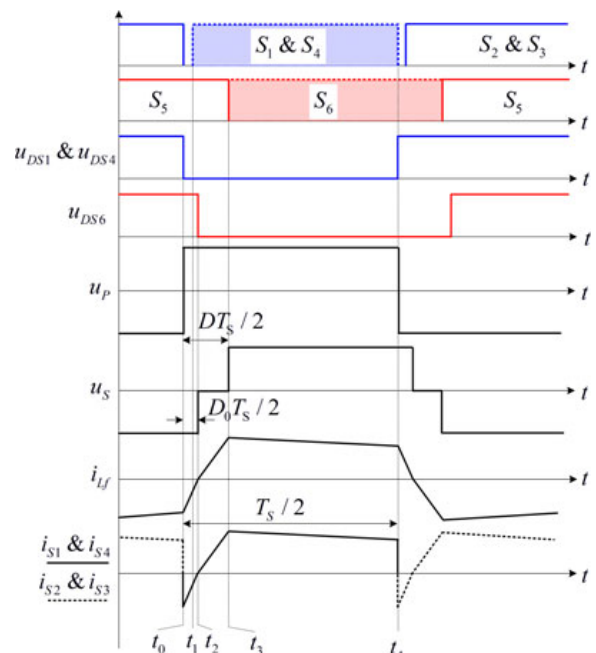


**Fig. 12. Key waveforms of the proposed converter in SS-CCM.**

As indicated by the waveforms of the essential side current, the converter has three operation modes, specifically optional side delicate exchanging nonstop conduction mode (SS-CCM), auxiliary side hard-exchanging consistent conduction mode (HS-CCM), and intermittent conduction mode (DCM), separately. 1) SS-CCM Operation: In SS-CCM, the converter can work in either the Buck mode ( $G < 1$ ), equalization mode ( $G = 1$ ), or Boost mode ( $G > 1$ ). The key waveforms of the FBC-VD-ABR operating in SS-CCM are appeared in Fig. 12, where  $D_0$  is characterized as the comparable obligation cycle amid which the essential current comes back to zero after the essential side switches turn OFF, and  $T_S$  is the exchanging time frame. There are eight phases in one exchanging period. Due to the symmetry of the circuit, only four stages are analyzed here and corresponding equivalent circuits for each operation stage are shown in Fig. 13.

**Stage 1 [ $t_0, t_1$ ] [see Fig. 13(a)]:**

Before  $t_0$ ,  $S_2$ ,  $S_3$ ,  $S_5$ , and  $D_2$  are ON. In any case, no present moves through  $S_5$  since body diode of  $S_6$  is opposite one-sided. At  $t_0$ ,  $S_2$ , and  $S_3$  turn OFF.

Body diodes of S1 and S4 start to direct because of the vitality put away in  $L_f$ , which brings about ZVS of S1 and S4. The vitality put away in  $L_f$  is conveyed to the information and  $C_{o2}$ . Because of the negative voltage over the inductor, the present  $i_{L_f}$  diminishes quickly

$$i_{L_f}(t) = i_{L_f}(t_0) + \frac{N U_o / 2}{L_f} (1/G + 1)(t - t_0). \quad (3)$$

**Stage 2 [ $t_1, t_2$ ] [see Fig. 13(b)]:**

At  $t_1$ ,  $S_1$  and  $S_4$  are turned ON with ZVS. This stage ends when  $i_{L_f}$  returns to zero, and  $D_2$  is OFF naturally without reverse recovery.

**Stage 3 [ $t_2, t_3$ ] [see Fig. 13(c)]:**

At  $t_2$ ,  $i_{L_f}$  returns to zero, the inductor  $L_f$  is charged by the input voltage

$$i_{L_f}(t) = i_{L_f}(t_2) + \frac{N U_o / 2}{G L_f} (t - t_2). \quad (4)$$

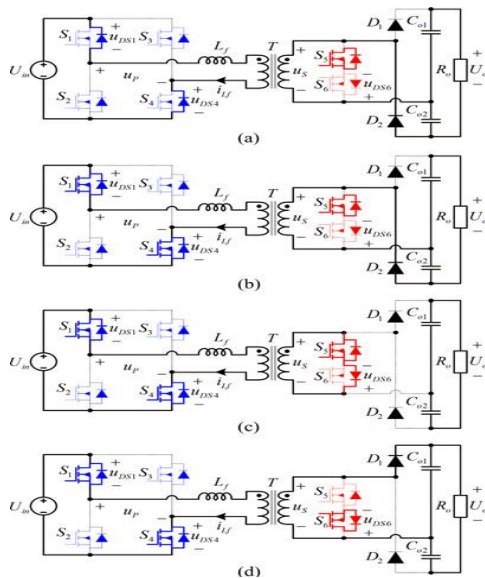


**Fig. 13. Equivalent circuits for each operation stage of SS-CCM: (a) Stage 1 [ $t_0, t_1$ ], (b) Stage 2 [ $t_1, t_2$ ], (c) Stage 3 [ $t_2, t_3$ ], and (d) Stage 4 [ $t_3, t_4$ ].**

**Stage 4 [ $t_3, t_4$ ] [see Fig. 13(d)]:**

At  $t_3$ ,  $S_5$  turns OFF and  $S_6$  is ON, but no current flows through  $S_6$ . Diode  $D_1$  begins to conduct.

The power is transferred to the load during this stage  
2) HS-CCM Operation: In SS-CCM, the auxiliary sideswitches commutate after  $i_{L_f}$  returns to zero, which means  $D > D_0$ . Once the optional side changes commutate before  $i_{L_f}$  returns to zero with  $D < D_0$ , the converter will enter the HS-CCM, in which the converter can just work in the Buck mode ( $G < 1$ ). The key waveforms of the FBC-VD-ABR operating in HS-CCM are appeared in Fig. 14. There are likewise eight stages in one exchanging period. Stage 1 [ $t_0, t_1$ ], Stage 2 [ $t_1, t_2$ ]: The operation standards and equivalent circuits of the two Stages are precisely the same as that of Stage 1 and Stage 2 in the SS-CCM mode. of Stage 1 and Stage 2 in the SS-CCM mode.

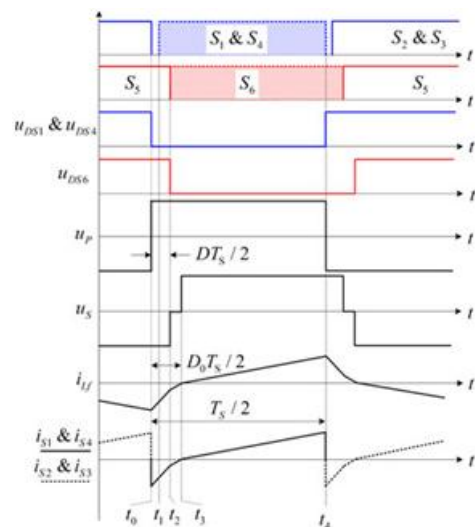


**Fig. 14. Key waveforms of the proposed converter in HS-CCM.**

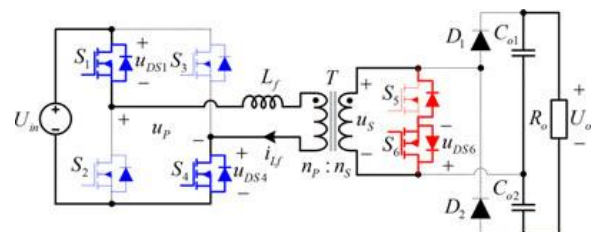


**Fig. 15. Equivalent circuit of Stage 3 in HS-CCM operation.**

**Stage 3 [ $t_2, t_3$ ]:**

At  $t_2$ , before  $i_{L_f}$  returns to zero,  $S_5$  is turned OFF and  $S_6$  is ON. The current through  $D_2$  is changed to flow through  $S_6$  and body diode of  $S_5$ .

All the two secondary switches, S5 and S6, and rectifier diode, D2, are hard switching. The equivalent circuit of this stage is shown in Fig. 15.

**Stage 4 [t3, t4]:**

The operation and equivalent circuit of this Stage are the same as that of Stage 4 in the SS-CCM mode. A similar operation works in the rest stages in a switching period.

**DCM Operation:**

In the event that the essential current has diminished to zero preceding the essential side switches commutate, the converter enters the DCM operation, in which the converter can just work in the Boost mode. The key waveforms of the FBC-VDABR working in DCM are appeared in Fig. 16. There are likewise eight phases in one exchanging period. Because of the symmetry of the circuit, just four phases are examined here and corresponding equivalent circuits for every operation stage are appeared in Fig. 17. Stage 1 [t0, t1] [see Fig. 17(a)]: Before t0, S2, S3, S5, are ON. Since  $i_{Lf} = 0$ , there is no vitality exchanged between the information and yield. At t0, S2 and S3 turn OFF with zero-voltage zero-current exchanging.

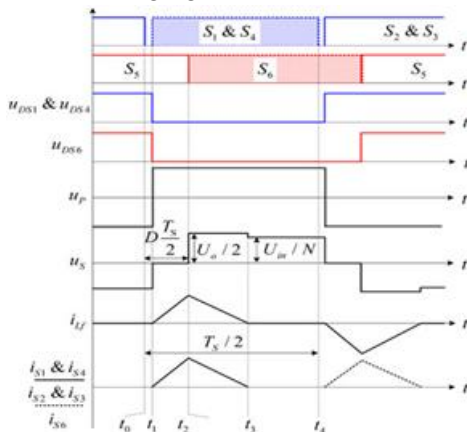


**Fig. 16. Key waveforms of the proposed converter in HS-CCM.**

**Stage 3 [t2, t3] [see Fig. 17(c)]:**

At t2, S5 turns OFF and S6 turns ON, but no current flows through S6. Diode D1 begins to conduct. The power is transferred to the load during this stage

$$i_{Lf}(t) = i_{Lf}(t_2) + \frac{1}{L_f} \int_{t_2}^t (U_o - U_o/2) dt \quad (8)$$

**Stage 5 [t3, t4] [see Fig. 17(d)]:**

At t4,  $i_{Lf}$  reaches zero.  $i_{Lf}$  will stay in a zero state in this stage and there is no energy transferred between the input and output.

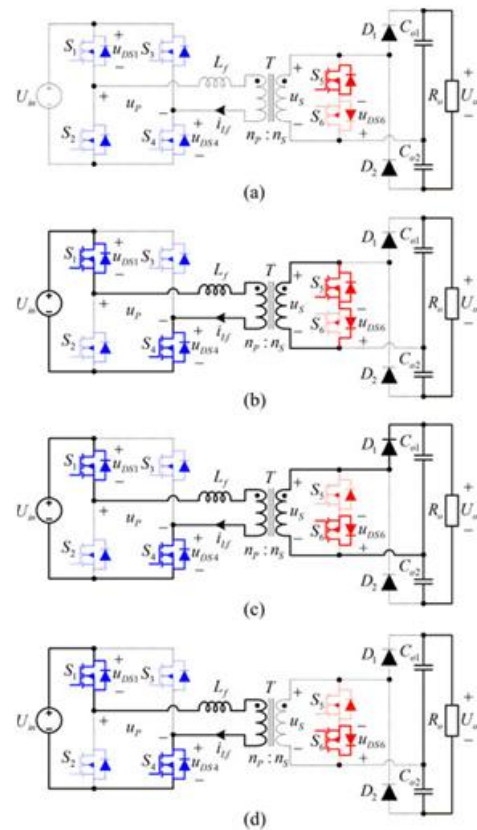


**Fig. 17. Equivalent circuits for each operation stage of DCM: (a) Stage 1 [t0, t1], (b) Stage 2 [t1, t2], (c) Stage 3 [t2, t3], and (d) Stage 4 [t3, t4].**

A similar operation works in the rest stages in a switching period.

**B. Output Characteristics**

According to the operational analysis of SS-CCM, the average primary current can be given by

$$I_{in} = \frac{i_{Lf}(t_0)}{2} D_0 + \frac{i_{Lf}(t_3)}{2} (D - D_0)$$

$$+ \frac{i_{Lr}(t_3) + i_{Lr}(t_4)}{2} (1-D). \quad (9)$$

Ignoring the power losses, then, the output power can be derived as

$$P_o = U_{in} I_{in}. \quad (10)$$

From (1)–(6), (9) and (10), the output power can be obtained as (11) shown at the bottom of the page. The same analysis process can be performed for HS-CCM and DCM. Based on the volt-second balance of inductor  $L_f$ , the boundary condition can be given by

$$D_{B1} = \frac{1-G}{2}. \quad (13)$$

Similarly, the boundary between the DCM and SS-CCM is determined by

$$D_{B2} = \frac{G-1}{G}. \quad (14)$$

Based on the analysis, the output characteristics of the FBC-VD-ABR are depicted in Fig. 18. Fig. 18(a) is the curves of normalized output power versus the duty cycle  $D$ , where output power is normalized.

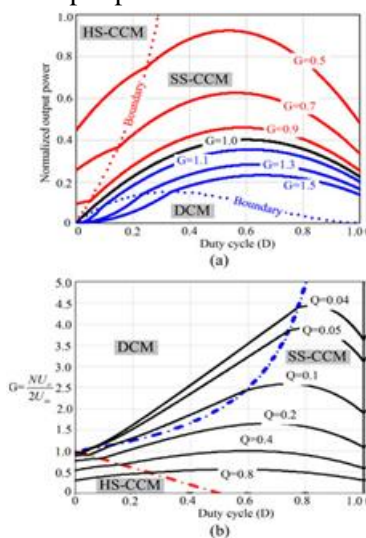


**Fig. 18. Output characteristics: (a) normalized output power versus duty cycle and (b) voltage gain versus duty cycle.**

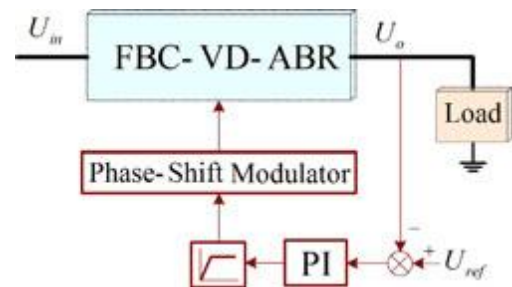


**Fig. 19. Control block diagram.**

Fig. 18(b) is the curves of voltage gain  $G$  versus the duty cycle. In these curves, the characteristic factor is defined as

$$Q = N^2 T_s R_o / 16L_f$$

where  $R_o$  is the load resistance. From these bends in Fig. 18, it can be seen that the yield power in the SS-CCM is more prominent than DCM and HS-CCM when the increase is the same. Then again, contrasted with the ordinary PWM converters, the addition bends, which are influenced chiefly by the obligation cycle and  $Q$  worth, are more like a thunderous converter. It can likewise be watched that HS-CCM just happens when the increase is littler than 1, which concurs with the investigation in past segment.

### C. Soft-Switching Characteristics:

As per the operation standards of the converter, the ZVS turn ON of all the essential side force MOSFETs can be accomplished when the converter works in the SS-CCM and HS-CCM modes. The ZVS turn OFF of essential side MOSFETs can likewise be gotten on account of the parasitic or parallel capacitors on the channel to wellspring of MOSFETs. At the point when the converter operates in the SS-CCM, ZVS turn-ON of the auxiliary side MOSFETs and zero current exchanging (ZCS) turn-OFF of rectifier diodes can likewise be accomplished. Be that as it may, when the converter works in HS-CCM, delicate exchanging of optional side gadgets will be lost. However, it ought to be noticed that, the turn-off loss of the optional side MOSFETs can be minimized in the HS-CCM on the grounds that the turn-off current is the base of these

three operation modes under the same yield power condition. Additionally, when the con-verter works in the DCM mode, ZCS can be accomplished for the essential switches and optional rectifier diodes, and ZVS can be achieved for the secondary-side MOSFETs. When analyzing the operation principles, the magnetizing in-ductance is ignored for simplicity. In fact, since the magnetizing current of the transformer is small, the extra conduction losses caused by the magnetizing current are quite small. What is more, the magnetizing current can help the primary-side MOSFETs to achieve ZVS more easily, whose principle is similar to the LLC resonant converter, especially in the low-power conditions. As a result, the circuit conversion efficiency can be improved.

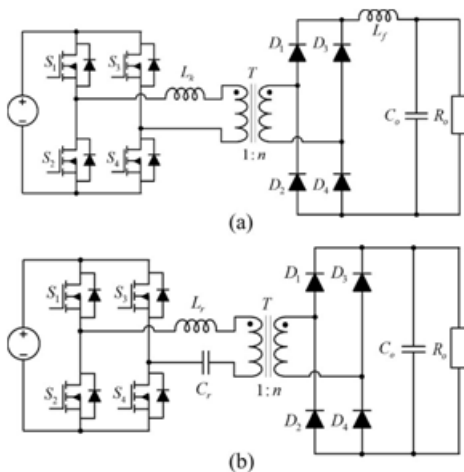


**Fig. 20.(a) Phase-shift full-bridge converter and (b) full-bridge LLC resonant converter.**

**D. Control Loop:**

According to the output characteristic curves shown in Fig. 18, the output voltage and power of the FBC-VD-ABR are regulated by the duty cycle defined in (2), which means the voltage and power can be regulated only by directly varying the phase shift angle  $\phi$ . Thus, the traditional voltage feedback loop can be adopted to regulate the output voltage, as shown in Fig. 19. The difference between the voltage reference and the sampled output voltage is used as the input of the PI regulator to generate the command value for the phase-shift modulator.

Since the control loop is very simple, it can be implemented with either analog circuit or digital signal processor.

**E. Performance Comparison:**

To help tradeoff design and topology selection in engineering applications, the performance comparison between the FBC-VD-ABR and other converters is necessary. Since the FBC-VD-ABR has a full-bridge input stage and it is suitable for high-power application, the conventional phase-shift FBC and the full-bridge LLC resonant converter [see Fig. 20(a) and (b)] are selected due to the similarity in structure and application, while others may not be suitable for comparison and are out of the scope of this paper.

**IV. EXPERIMENTAL RESULTS**

A 1 kW model controlled by a MC56F8247 computerized signal processor is worked to confirm the hypothetical investigation. The converter is intended for a stand-alone renewable force framework, and utilized as the front-end converter of an inverter. The particulars are recorded in Table II. The information voltage is 110–160 V, and the yield voltage is 380 V. Fig. 21 demonstrates the voltage  $u_{p,uS}$ , and current  $i_{L f}$  wave-types of the FBC-VD-ABR under DCM, SS-CCM, and HS-CCM, individually. As appeared in Fig. 21(a) and (b), the primary current declines directly when the information force is trans-ferred to the yield side through the channel inductor, in light of the fact that thenormalized voltage pick up  $G$  is more noteworthy than 1 and the converter works in the Buck mode. In Fig. 21(a), when the inductor dog rent abatements to zero, a little voltage ringing can be seen on the auxiliary twisting of the transformer, which is brought about by the parasitic parameters. Then again, the essential current increments straightly amid the force exchanging state, as appeared in Fig. 21(c), with voltage pick up  $G < 1$ . The waveforms in Fig. 21 fulfill the hypothetical examination truly well. The exchanging waveforms of the essential and optional side switches under various operation modes are appeared in Figs. 22– 24.

As appeared in Fig. 22, when the converter works in the DCM, ZVS execution is lost while ZCS execution can be refined for the essential side switches, and ZVS execution is accomplished for the optional side switches under the DCM. Since all the essential switches work in the same example and both the two auxiliary side switches work symmetrically, ZCS and ZVS are expert for all the essential side switches and optional side switches, individually. The waveforms indicated in Fig. 24 show that ZVS can be accomplished for all the essential and auxiliary side switches when the converter works under the SS-CCM. In any case, from the waveforms of Fig. 24, it can be seen that ZVS execution must be accomplished for the essential side switches when the converter works in the HS-CCM, and the optional side switches work with hard-exchanging. Yet, it ought to be noticed that, the turn-ON/OFF current of the auxiliary side switches is amazingly little in the HS-CCM.

**TABLE II: COMPONENTS AND PARAMETERS OF THE PROTOTYPE**

Components	Parameters
Input voltage ( $U_m$ )	110V~160V
Output voltage ( $U_o$ )	380V
Maximum output power ( $P_o$ )	1000W
Maximum input current ( $I_m$ )	8A
Switching frequency	80kHz
Turns ratio of transformer ( $n_p:n_s$ )	9:11
Inductor $L_f$	16μH
Primary side MOSFETs	IRFS4227
Secondary side MOSFETs	FQA38N30
Secondary side diodes	DSEC30-06A
Output capacitors ( $C_{o1}, C_{o2}$ )	330μF

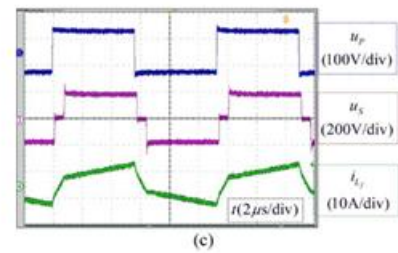
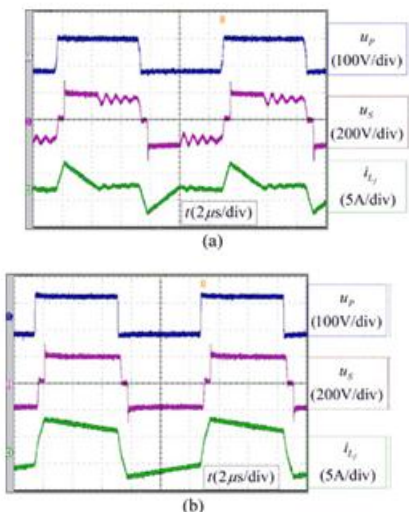


**Fig. 21. Voltage  $u_p, u_s$ , and current  $i_{L_f}$  waveforms in (a) discontinuous-conduction mode, (b) soft-switching continuous-conduction mode, and (c) hard-switching continuous-conduction mode.**

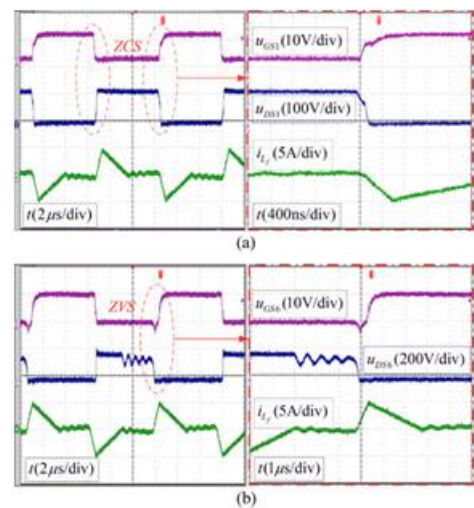


**Fig. 22. Switching waveforms of (a) primary-side switch and (b) secondary-side switch under discontinuous-conduction mode.**

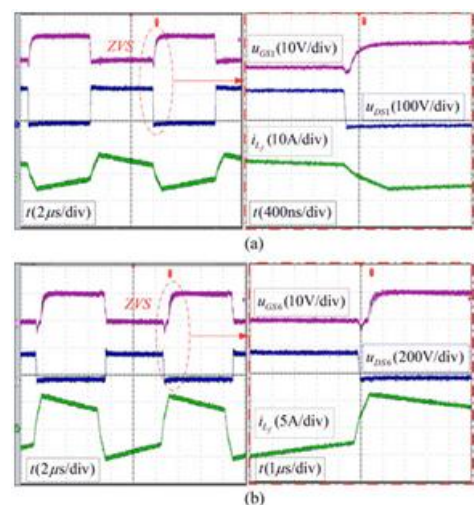


**Fig. 23. Switching waveforms of (a) primary-side**

switch and (b) secondary-side switch under soft-switching continuous-conduction mode.

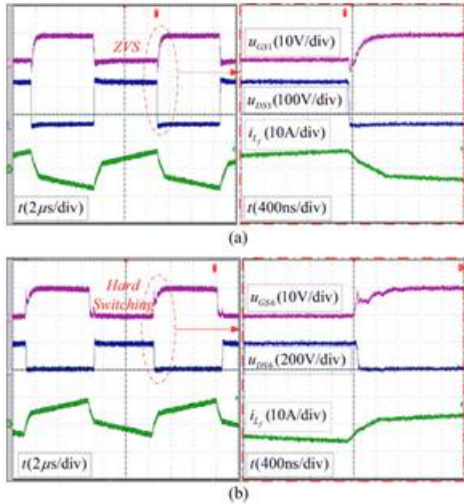


Fig. 24. Switching waveforms of (a) primary-side switch and (b) secondary-side switch under hard-switching continuous-conduction mode.

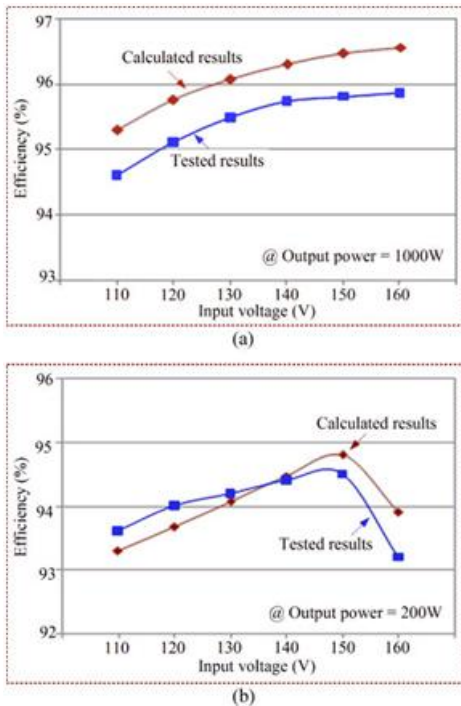


Fig. 25. Efficiency comparison: (a) output power  $P_o = 1000$  W and (b) output power  $P_o = 200$  W

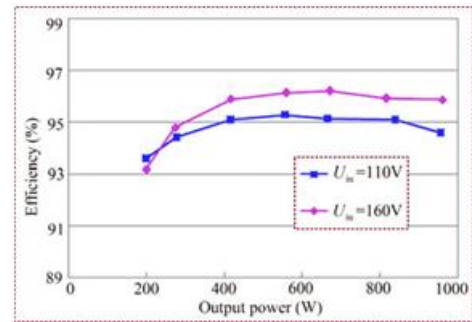


Fig. 26. Measured efficiency versus output power.

Fig. 25 demonstrates the deliberate and computed efficiencies of the proposed FBC-VD-ABR under various info voltages. The yield force of Fig. 25(a) is 1000 W, while Fig. 25(b) is 200 W yield. At the point when the yield force is 1000 W, the converter works in the SS-CCM and delicate exchanging can be accomplished for all the force gadgets. In this manner, the significant force misfortune is the conduction misfortune, which makes the bends up with the info voltage expanding. It ought to be noticed that the misfortunes brought on by the PCB lines and connectors are excluded in the count. At the point when the yield force is 200 W and the info voltage is lower than 160 V, the converter works in the DCM and the conduction misfortune is the real influence misfortune too. Subsequently, the higher the info voltage, the higher the effectiveness.

Nonetheless, when the information voltage is 160 V, the converter works in the HS-CCM, the MOSFETs and the diodes on the auxiliary side work under hard changing, which prompts higher exchanging misfortune. Thus, the proficiency drops down. The proficiency bends versus yield power under 160 and 110 V information voltages are appeared in Fig. 26. At the point when the info voltage is 160 V, the pinnacle effectiveness is around 96.4% and the productivity at full load is around 95.8%. At the point when the info voltage is 110 V, the greatest effectiveness is around 95.3% and the productivity at full load is around 94.6%. It can be seen that productivity of more than 95% is accomplished in a wide power and voltage ranges with the proposed converter.

## V. CONCLUSION:

In this paper, a group of delicate exchanging dc–dc converters has been exhibited for high-effectiveness applications taking into account the novel proposed ABRs. In the proposed converters, all the force switches are worked at altered half obligation cycle, and the yield voltage direction is accomplished by embracing stage shift control between the essential and optional side switches. ZVS execution has been accomplished for both the essential and optional side switches in a wide voltage and burden range. Moreover, the converse recuperation issues connected with the rectifier diodes are lightened. In this way, the exchanging misfortunes of the proposed converters can be decreased, which is vital for high-recurrence, high-proficiency, and high-influence thickness applications.

In addition, the spillage inductance of the transformer has been used as the vitality exchange inductor, and every one of the gadgets voltages are cinched to the info or yield voltage. Hence, the voltage overshoots on the gadgets are viably smothered. Furthermore, the proposed converters are appropriate for wide-run applications since they can work either in Buck or Boost mode. For instance, the FBC with VD ABR is broke down with operation standards and yield qualities exhibited. Trial consequences of a 1 kW model have confirmed the achievability and adequacy of the proposed topological philosophy and converters.

## REFERENCES:

- [1] M. Yilmaz and P. T. Krein, "Review of the impact of vehicle-to-grid technologies on distribution systems and utility interfaces," *IEEE Trans. Power Electron.*, vol. 28, no. 12, pp. 5673–5689, Dec. 2013.
- [2] M. Yilmaz and P. T. Krein, "Review of battery charge topologies, charging power levels, and infrastructure for plug-in electric and hybrid vehicles," *IEEE Trans. Power Electron.*, vol. 28, no. 5, pp. 2151–2169, May 2013.
- [3] Y. H. Kim, S. C. Shin, J. H. Lee, Y. C. Jung, and C. Y. Won, "Soft-switching current-fed push-pull converter for 250-W AC module applications," *IEEE Trans. Power Electron.*, vol. 29, no. 2, pp. 863–872, Feb. 2014.
- [4] X. Pan and A. K. Rathore, "Novel interleaved bidirectional snubberless soft-switching current-fed full-bridge voltage doubler for fuel-cell vehicles," *IEEE Trans. Power Electron.*, vol. 28, no. 12, pp. 5535–5546, Dec. 2013.
- [5] W. J. Lee, G. E. Kim, G. W. Moon, and S. K. Han, "A new phase-shifted full-bridge converter with voltage-doubler-type rectifier for high efficiency PDP sustaining power modules," *IEEE Trans. Ind. Electron.*, vol. 55, no. 6, pp. 2450–2458, Jun. 2008.
- [6] W. Yu, J. S. Lai, W. H. Lai, and H. Wan, "Hybrid resonant and PWM converter with high efficiency and full soft-switching range," *IEEE Trans. Power Electron.*, vol. 27, no. 12, pp. 4925–4833, Dec. 2012.
- [7] H. Y. Cha, L. H. Chen, R. J. Ding, Q. S. Tang, and F. Z. Peng, "An alternative energy recovery clamp," *IEEE Trans. Power Electron.*, vol. 23, no. 6, pp. 2828–2837, Nov. 2008.
- [8] D. S. Gautam and A. K. S. Bhat, "A comparison of soft-switched dc-to-dc converters for electrolyzer application," *IEEE Trans. Power Electron.*, vol. 28, no. 1, pp. 54–62, Jan. 2013.
- [9] Z. Chen, S. Liu, and L. Shi, "A soft switching full bridge converter with reduced parasitic oscillation in a wide load range," *IEEE Trans. Power Electron.*, vol. 29, no. 2, pp. 801–811, Feb. 2014.
- [10] W. Chen, X. Ruan, and R. Zhang, "A novel zero-voltage-switching PWM full bridge converter," *IEEE Trans. Power Electron.*, vol. 23, no. 2, pp. 793–801, Feb. 2008.

- [11] Y. S. Shin, C. S. Kim, and S. Y. Han, "A pulse-frequency-modulated full-bridge DC-DC converter with series boost capacitor," *IEEE Trans. Ind. Electron.*, vol. 58, no. 11, pp. 5154–5162, Nov. 2011.
- [12] I. Lee and G. W. Moon, "Soft-switching DC/DC converter with a full ZVS range and reduced output filter for high-voltage applications," *IEEE Trans. Power Electron.*, vol. 28, no. 1, pp. 112–122, Jan. 2013.
- [13] K. M. Cho, Y. D. Kim, I. H. Cho, and G. W. Moon, "Transformer integrated with additional resonant inductor for phase-shift full-bridge converter with primary clamping diodes," *IEEE Trans. Power Electron.*, vol. 27, no. 5, pp. 2405–2414, May 2012.
- [14] B. Gu, C. Y. Lin, B. Chen, J. Dominic et al., "Zero-voltage-switching PWM resonant full-bridge converter with minimized circulating losses and minimal voltage stresses of bridge rectifiers for electric vehicle battery chargers," *IEEE Trans. Power Electron.*, vol. 28, no. 10, pp. 4657–4667, Oct. 2013.
- [15] T. Mishima, K. Akamatsu, and M. Nakaoka, "A high frequency-link secondary-side phase-shifted full-range soft-switching PWM DC-DC converter with ZCS active rectifier for EV battery charges," *IEEE Trans. Power Electron.*, vol. 28, no. 12, pp. 5758–5773, Dec. 2013.
- [16] A. K. Jain and R. Ayyanar, "PWM control of dual active bridge: Comprehensive analysis and experimental verification," *IEEE Trans. Power Electron.*, vol. 26, no. 4, pp. 1215–1227, Apr. 2011.
- [17] G. G. Oggier, G. O. Carcia, and A. R. Oliva, "Modulation strategy to operate the dual active bridge DC-DC converter under soft switching in the whole operating range," *IEEE Trans. Power Electron.*, vol. 26, no. 4, pp. 1228–1236, Apr. 2011.
- [18] B. Zhao, Q. Song, and W. Liu, "Power characterization of isolated bidirectional dual-active-bridge DC-DC converter with dual-phase-shift control," *IEEE Trans. Power Electron.*, vol. 27, no. 9, pp. 4172–4176, Sep. 2012.
- [19] H. Koek, M. Neubert, and R. W. Doncker, "Enhanced modulation strategy for a three-phase dual active bridge—boosting efficiency of an electric vehicle converter," *IEEE Trans. Power Electron.*, vol. 28, no. 12, pp. 5499–5507, Dec. 2013.
- [20] W. Feng, F. C. Lee, and P. Mattavelli, "Optimal trajectory control of LLC resonant converters for LED PWM dimming," *IEEE Trans. Power Electron.*, vol. 29, no. 2, pp. 979–987, Feb. 2014.
- [21] I. O. Lee and G. W. Moon, "The k-Q analysis for an LLC series resonant converter," *IEEE Trans. Power Electron.*, vol. 29, no. 1, pp. 13–16, Jan. 2014.
- [22] X. Fang, H. Hu, F. Chen, U. Somani, E. Auadisiyan, J. Shen, and I. Batarseh, "Efficiency-oriented optimal design of the LLC resonant converter based on peak gain placement," *IEEE Trans. Power Electron.*, vol. 28, no. 5, pp. 2285–2296, May 2013.
- [23] Y. Ren, M. Xu, J. Sun, and F. C. Lee, "A family of high power density unregulated bus converters," *IEEE Trans. Power Electron.*, vol. 20, no. 5, pp. 1045–1054, Sep. 2005.
- [24] B. Su and Z. Lu, "An interleaved totem-pole boost bridgeless rectifier with reduced reverse-recovery problems for power factor correction," *IEEE Trans. Power Electron.*, vol. 25, no. 6, pp. 1406–1415, Jun. 2010.



- [25] Y. S. Roh, Y. J. Moon, J. Park, and C. Yoo, "A two-phase interleaved power factor correction boost converter with a variation-tolerant phase shifting technique," *IEEE Trans. Power Electron.*, vol. 29, no. 2, pp. 1032–1040, Feb. 2014.
- [26] B. Lu, C. Wang, F. C. Lee, N. Lee, and Y. Yu, "A high frequency ZVS isolated dual boost converter with holdup time extension," in *Proc. 37th IEEE Power Electron. Spec. Conf.*, 2006, pp. 1–6.
- [27] W. Li, S. Zong, F. Liu, H. Yang, X. He, and B. Wu, "Secondary-side phase-shift-controlled ZVS DC/DC converter with wide voltage gain for high input voltage applications," *IEEE Trans. Power Electron.*, vol. 28, no. 11, pp. 5128–5139, Nov. 2013.